

**Supporting information for**

**Bioinspired Hole-Conducting Polymers for Application in  
Organic Light-Emitting Diodes**

Chih-Chia Cheng,<sup>a</sup> Yu-Lin Chu,<sup>a</sup> Pei-Hsiu Huang,<sup>a</sup> Ying-Chieh Yen,<sup>a</sup> Chih-Wei Chu,<sup>bc</sup>  
Arnold C.-M. Yang,<sup>d</sup> Fu-Hsiang Ko,<sup>e</sup> Jem-Kun Chen<sup>f</sup> and Feng-Chih Chang<sup>\*ag</sup>

<sup>a</sup> Institute of Applied Chemistry, National Chiao-Tung University, 30050 Hsinchu, Taiwan

<sup>b</sup> Research Center for Applied Sciences, Academia Sinica, Taipei, 11529, Taiwan

<sup>c</sup> Department of Photonics, National Chiao-Tung University, Hsinchu, 30050, Taiwan

<sup>d</sup> Department of Materials Science and Engineering, National Tsing-Hua University, Hsinchu, 30050, Taiwan

<sup>e</sup> Department of Materials Science and Engineering, National Chiao-Tung University, Hsinchu 30050, Taiwan

<sup>f</sup> Department of Materials Science and Engineering, National Taiwan University of Science and Technology, Taipei 10607, Taiwan

<sup>g</sup> R&D Center for Membrane Technology, Chung Yuan Christian University, Chungli, Taoyuan 32043, Taiwan

	Pages
<b>Index</b>	<b>S1</b>
<b>Experimental Section</b>	<b>S2</b>
<b>Syntheses</b>	<b>S5</b>
<b>Variable Temperature FTIR Experiments</b>	<b>S11</b>
<b><sup>1</sup>H-NMR Titration Experiments</b>	<b>S13</b>
<b>Solvent Resistance Experiments</b>	<b>S14</b>
<b>OLED Devices</b>	<b>S16</b>
<b>References</b>	<b>S19</b>

## Experimental Section

### Materials

High-regioregular poly(3-hexylthiophene) (HR-PU) was purchased from FEM. All other chemicals were purchased from Aldrich (USA) or Acros Organics (Germany) and were used as received. All solvents were purchased from TEDIA (USA) and distilled over CaH<sub>2</sub> prior to use.

### Characterizations

**Fourier Transform Infrared (FT-IR) spectra** were obtained from Nicolet Avatar 320 FT-IR spectrometer; 32 scans were collected with a spectral resolution of 1 cm<sup>-1</sup>. The conventional KBr disk method was employed. Sample was dissolved in DMF and then cast onto a KBr disk and dried in vacuum at 120 °C for 24 h.

**Nuclear Magnetic Resonance (NMR) measurement.** <sup>1</sup>H-NMR spectra were recorded using a Varian Inova- 300 MHz spectrometer equipped with a 9.395 T Bruker magnet. Samples of ca. 5 mg were analyzed at 25 °C in deuterated solvent. <sup>13</sup>C-NMR spectra were performed on a Varian Inova- 300 MHz spectrometer operated at 75 MHz. All samples of ca. 20 mg were dissolved in deuterated solvent and analyzed at 25 °C

**Gas Chromatography/Mass Spectrometry.** GC/MS spectra were acquired using a Micromass Trio 2000 mass spectrometer (Micromass, Beverly, MA).

**Differential Scanning Calorimetry (DSC).** DSC was performed using a TA DSC-Q20 controller operated under a dry nitrogen atmosphere. The samples were weighed (ca. 5–10 mg), sealed in an aluminum pan, and then heated from -10 to +250

°C at a rate of 10 °C/min.

**Wide-Angle X-ray Diffraction (WAXD).** WAXD patterns of powders were obtained using a Rigaku D/max-2500 X-ray diffractometer. The radiation source was Ni-filtered Cu K $\alpha$  radiation at a wavelength of 0.154 nm. The voltage and current were set at 30 kV and 20 mA, respectively. The sample was mounted on a circular sample holder; the data were collected by a proportional counter detector over the  $2\theta$  range from 2 to 50° at a rate of 5° min $^{-1}$ . Bragg's law ( $\lambda = 2d \sin\theta$ ) was used to compute the  $d$ -spacing corresponding to the complementary behavior.

**UV–Vis and Photoluminescence (PL) Spectra.** UV–Vis and photoluminescence (PL) spectra were measured using an HP 8453 diode-array spectrophotometer and a Hitachi F-4500 luminescence spectrometer, respectively.

**Cyclic voltammetry (CV) measurements** were performed using a BAS 100 B/W electrochemical analyzer operated at a scan rate of 100mV s $^{-1}$ . The potentials were measured against a Ag/Ag $^{+}$  (0.01 M AgNO<sub>3</sub>) reference electrode using ferrocene/ferrocenium (Fc/Fc $^{+}$ ) as an internal standard.

**Atomic Force Microscopy (AFM).** Height measurements of the microcapsules were determined using tapping-mode AFM (Digital Instrument NS4/D3100CL/Multi-Mode AFM; Veeco-Digital Instruments, Santa Barbara, CA) with silicon cantilevers (Pointprobe Silicon AFM Probe) at 25 °C in air. Sample preparation for AFM imaging was spin-coated onto the indium-tin oxide (ITO) surface.

**Fabrication of OLEDs:** The EL devices were fabricated through vacuum deposition

of the materials at 10<sup>-6</sup> torr onto ITO glass having a sheet resistance of 25 Ω square<sup>-1</sup>. All of the organic layers were deposited at a rate of 1.0 Å s<sup>-1</sup>. The cathode was completed through thermal deposition of LiF at a deposition rate of 0.1 Å s<sup>-1</sup>, and then capped with Al metal through thermal evaporation at a rate of 4.0 Å s<sup>-1</sup>. The relationships of the current density and brightness of the devices with respect to voltage were measured using a Keithley 2400 source meter and a Newport 1835C optical meter equipped with an 818ST silicon photodiode. The EL spectrum was obtained using a Hitachi F4500 luminescence spectrometer.

## Syntheses

### Synthesis of uracil-functionalized thiophene monomer

3-Bromohexylthiophene<sup>1</sup> (1.97 g, 8.00 mmol) and anhydrous potassium carbonate (1.08 g, 7.8 mmol) were added to a solution of uracil (0.90 g, 8.00 mmol) in DMF and then the resulting suspension was stirred at 60 °C for 24 h. The insoluble material obtained was filtrated out, washed with water, and recrystallized twice from toluene. Yield: 1.09g (49%); FAB-MS: m/z (%) = 279; <sup>1</sup>H NMR (300 MHz, CDCl<sub>3</sub>): δ = 1.34 (m, 4H), 1.65 (br, 2H), 2.60 (m, 2H), 3.68 (t, 2H), 5.65 (d, 1H), 6.89 (d, 1H), 7.08 (d, 1H), 7.21 (d, 1H), 8.80 (s, 1H); <sup>13</sup>C NMR (300 MHz, CDCl<sub>3</sub>): δ = 26.45, 28.96, 29.19, 30.30, 30.49, 49.06, 102.34, 120.17, 125.45, 128.40, 142.96, 144.65, 151.15, 164.18.

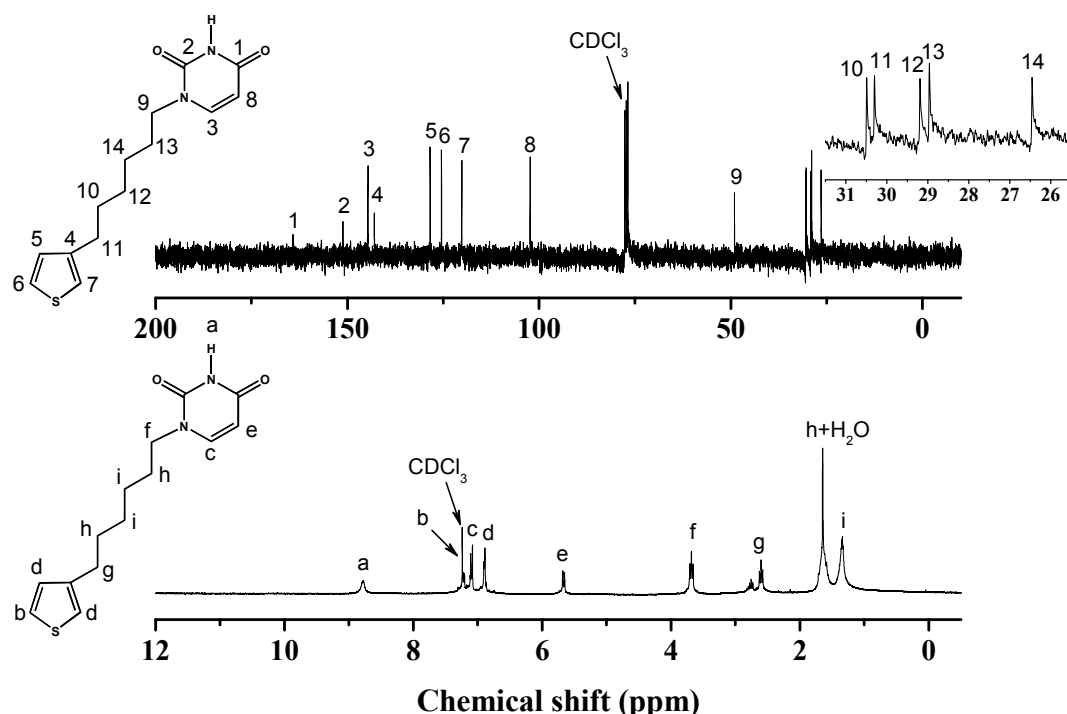


**Figure S1.** <sup>1</sup>H-NMR and <sup>13</sup>C-NMR spectra of uracil-functionalized thiophene in CDCl<sub>3</sub>.

## Synthesis of low-regioregular polythiophene containing pendant uracil groups (LR-PU)

Uracil-functionalized thiophene (1g, 3.60 mmol) and anhydrous  $\text{FeCl}_3$  (3.81 g, 23.50 mmol) was dissolved in dry chloroform (15 mL) and then solution was purged with dry argon for 10 min. The solutions were degassed through three freeze/thaw evacuation cycles. Subsequently, the mixture was reacted for 12h at room temperature and poured into methanol (200 mL) to precipitate the polymer. The crude polymer was filtered, further purified by extraction in a Soxhlet extractor with refluxing methanol for 48 h, and dried under vacuum, Yield: 0.72 g (72%).  $^1\text{H}$  NMR (300 MHz, *d*6-DMSO):  $\delta$  = 1.23 (br, 2H), 1.52 (br, 2H), 2.71 (t, 2H), 2.87 (t, 2H), 3.47 (t, 2H), 5.48 (d, 1H), 7.07(s, 1H), 7.57 (d, 1H), 11.17 (s, 1H).

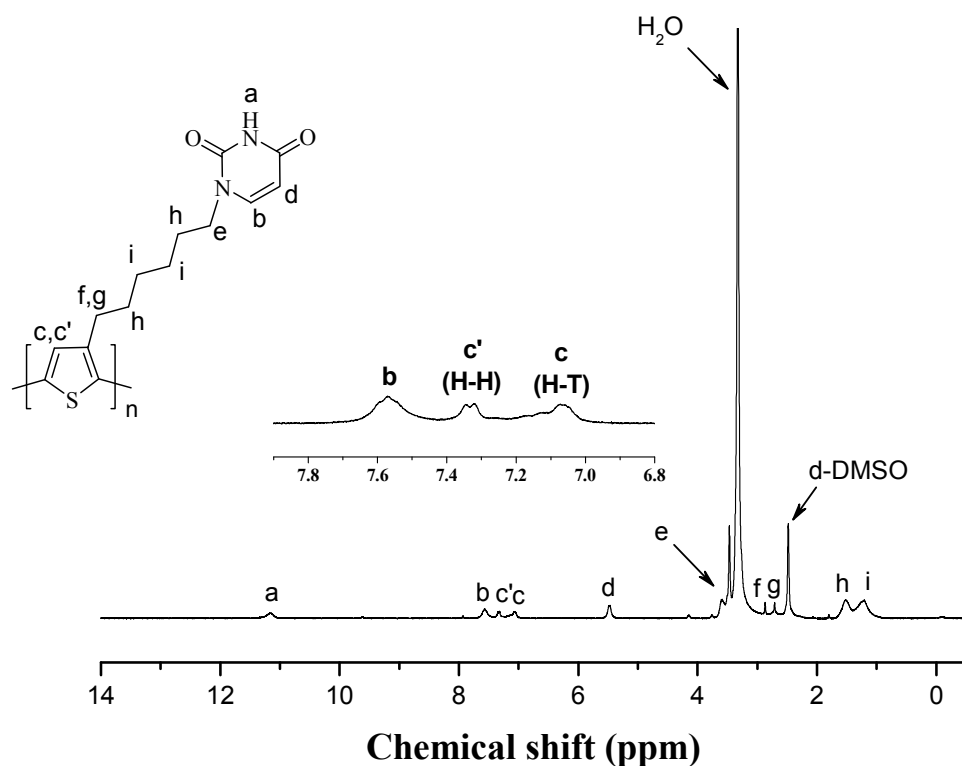


**Figure S2a.**  $^1\text{H}$ -NMR spectrum of LR-PU in *d*6-DMSO.

### Synthesis of low-regioregular P3HT-co-PU random copolymer (LR-PU31)

The preparation of the LR-PU31 derivatives was prepared by similar procedure to that described for LR-PU using compound 1 (0.34g, 1.20 mmol) and 3-hexylthiophene (0.41 g, 2.40 mmol) instead of compound 1, yield: 0.64g (85%).  $^1\text{H}$  NMR (300 MHz,  $\text{CDCl}_3$ ):  $\delta$  = 0.88 (t, 3H), 1.32 (br, 12H), 1.57 (br, 4H), 2.54 (t, 4H), 2.78 (t, 4H), 3.69 (t, 2H), 5.67 (d, 1H), 6.96 (d, 2H), 7.09 (br, 1H), 9.48 (br, 1H). Repeating unit of  $^1\text{H}$ -NMR analysis showed a 3:1 (P3HT:PU) ratio.

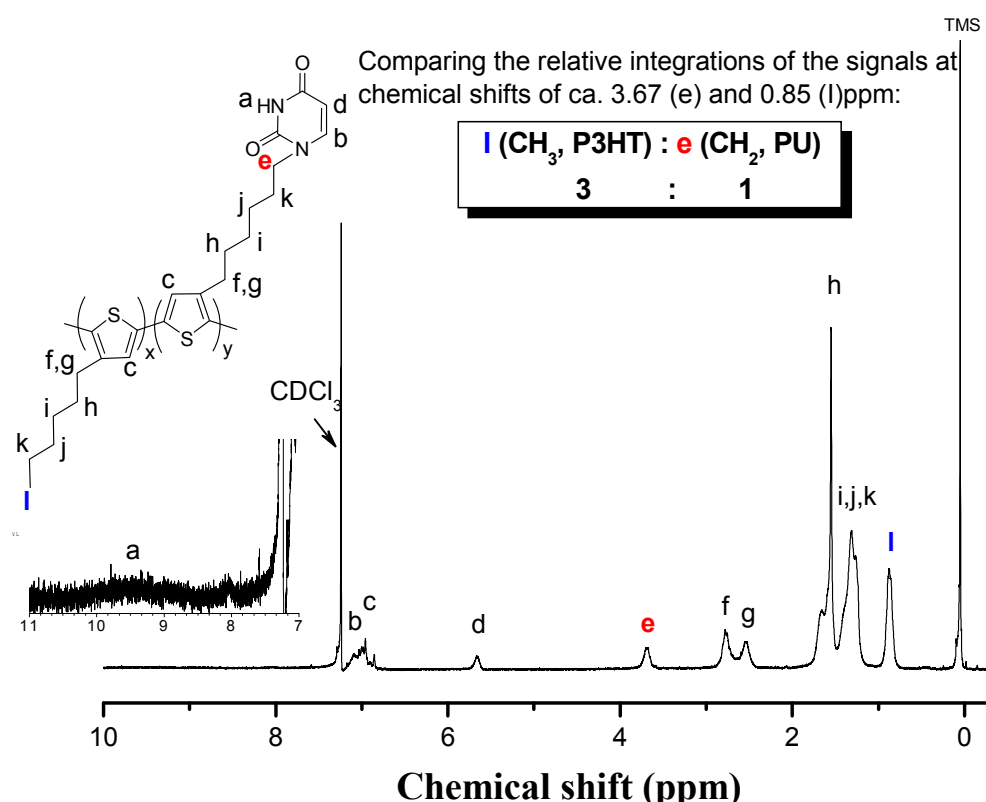


**Figure S2b.**  $^1\text{H}$ -NMR spectrum of LR-PU31 in  $\text{CDCl}_3$ .

## Synthesis of high-regioregular polythiophene containing pendant uracil groups (HR-PU)

High-regioregular poly(3-hexyl azide thiophene) (HT-N3-P3HT) was synthesized from High-regioregular poly(3-bromohexylthiophene) according to the procedures described previously.<sup>1</sup> Propargyl uracil<sup>2</sup> (0.75 g, 5.00 mmol) and HT-N3-P3HT (0.52 g, 0.04 mmol) were dissolved in DMF (10mL)/THF (5 mL) and then the resulted solution was purged with a dry argon atmosphere for 10 min. N,N',N'',N''-pentamethyldiethylenetriamine (PMDETA; 41.7  $\mu$ L, 0.02 mmol) was added via syringe, leading the mixture to becoming homogeneous and then the solution was degassed through three freeze/thaw evacuation cycles. Upon the addition of CuBr (0.002 g, 0.02 mmol), the color of the solution was gradually changed from light blue to light green. The solution was heated to 50 °C with stirring under an argon atmosphere until the azide peak ( $2092\text{ cm}^{-1}$ ) completely disappeared (8h) as observed through the FTIR spectrum. After cooling to 25 °C, the reaction mixture was passed through an aluminum oxide column to remove the Cu(II) catalyst. The solution was transferred to a dialysis bag and subjected to dialysis at room temperature for 3 d. Finally, the solvent was evaporated, and the residue was purified by precipitation into methanol; it was then filtrated and dried under vacuum. yield: 0.15 g (29%).  $^1\text{H}$  NMR (300 MHz, *d*6-DMSO):  $\delta$  = 1.25 (br, 4H), 1.59 (br, 2H), 1.77 (br, 2H), 2.72 (t, 2H), 4.30 (t, 2H), 4.89 (d, 1H), 7.14 (s, 1H), 7.70 (s, 1H), 8.04 (d, 1H), 11.27 (s, 1H).

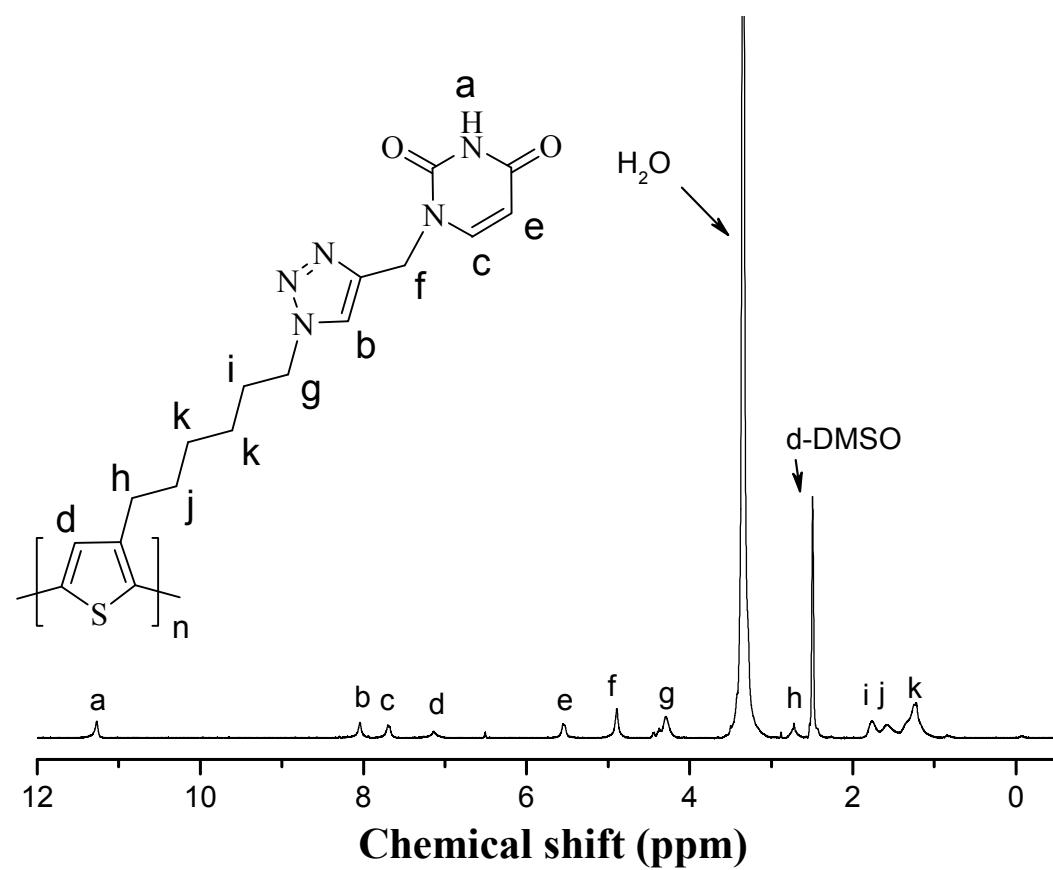


**Figure S3.**  $^1\text{H}$ -NMR spectrum of of HR-PU in  $d_6$ -DMSO.

**Table S1.** Summary of molecular weights (Mw), polydispersity index (PDI), and regioregularity (RR) for the uracil-functioned polymers, LR-P3HT and HR-P3HT.

Polymers	Mw <sup>a</sup>	PDI <sup>a</sup>	RR (%) <sup>b</sup>
HR-P3HT	16900	2.675	98
LR-P3HT	19235	2.055	72
LR-PU31	17569	2.145	56
LR-PU	11648	1.774	47
HR-PU	20959	1.564	98

<sup>a</sup> The average molecular weights (Mw) and PDI of the polymers were determined through gel permeation chromatography (GPC).

<sup>b</sup> The regioregularity (RR) was calculated from the <sup>1</sup>H NMR spectra by comparing the relative integrations of the signals at chemical shifts of ca. 2.7-2.8 (head-to-tail, H-T) and 2.4-2.5 (head-to-head, H-H) ppm, as shown in the following figure.

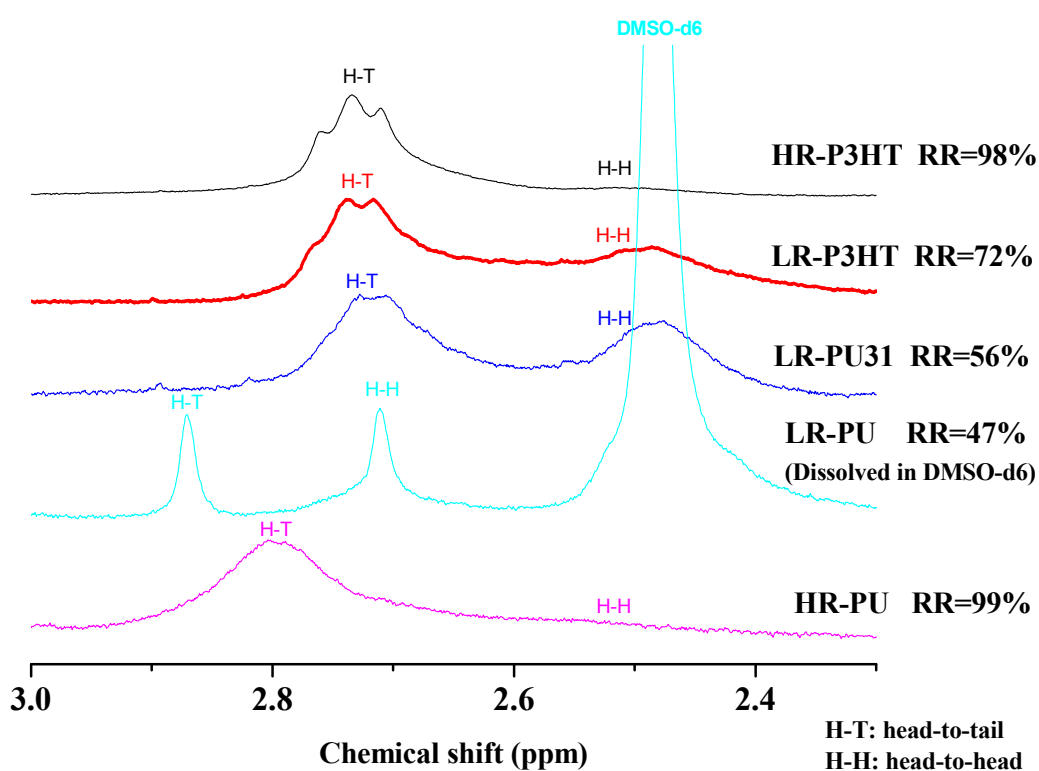


**Figure S4.** The  $\alpha$ -methylene region of the <sup>1</sup>H NMR spectra for the uracil-functioned polymers, LR-P3HT and HR-P3HT.

## Variable Temperature FTIR Experiments

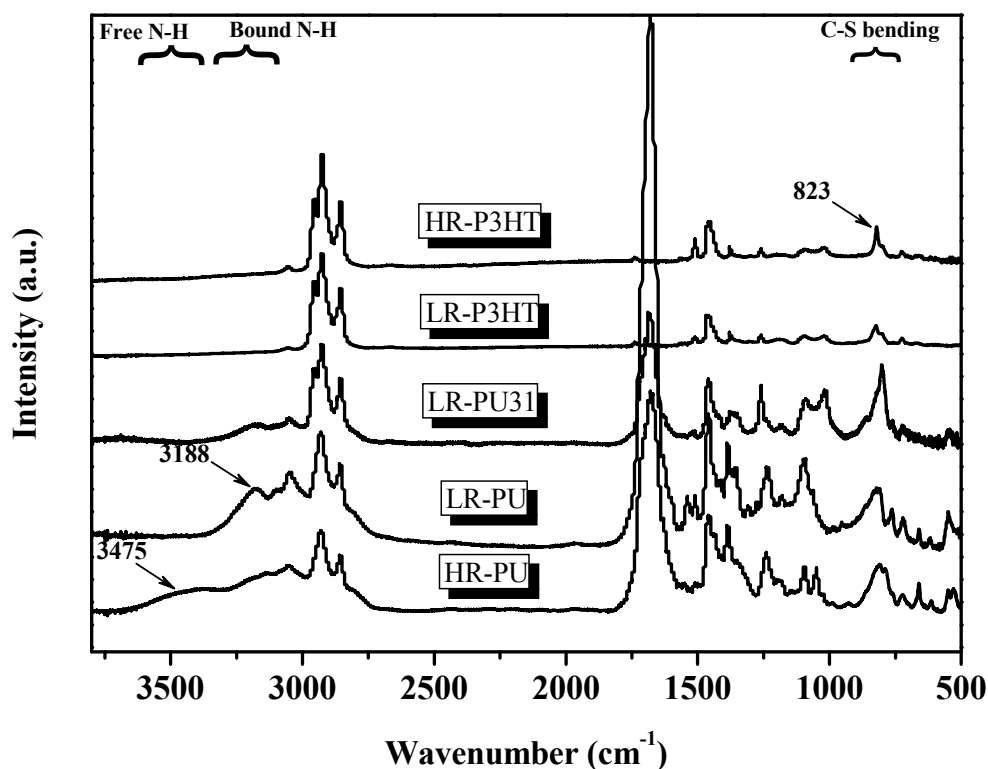


**Figure S5.** FTIR spectra recorded at room temperature in the range  $500\text{-}3750\text{ cm}^{-1}$  for the uracil-functioned polymers, LR-P3HT and HR-P3HT.

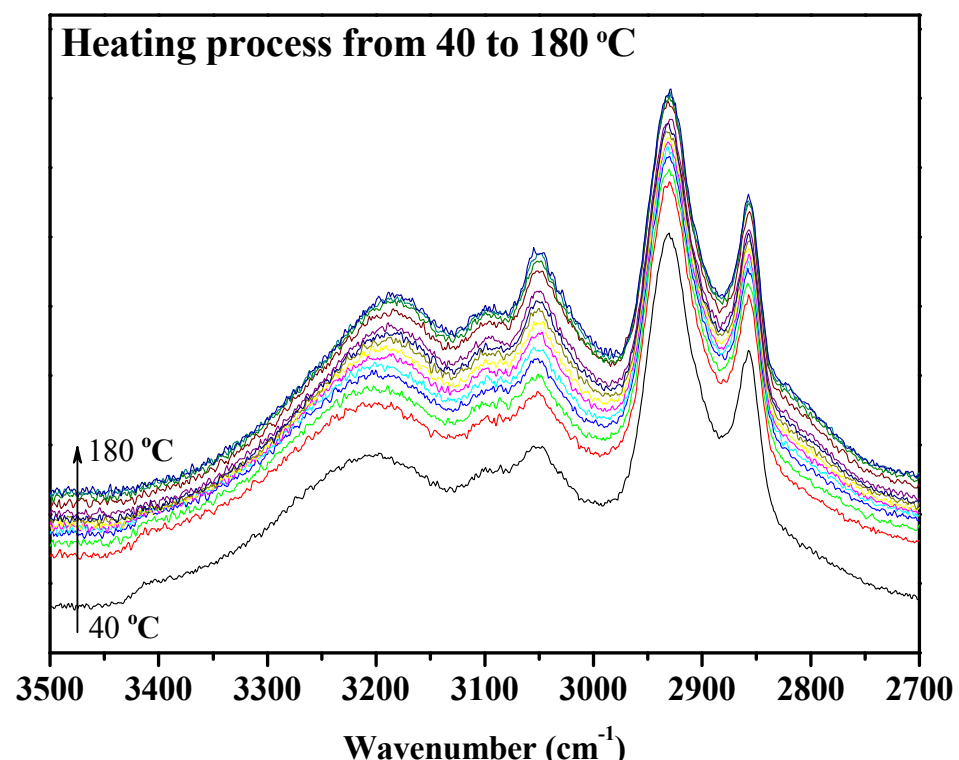


**Figure S6** Variable-temperature FT-IR spectra of LR-PU recorded in the range 2700–3500 cm<sup>-1</sup>.

## <sup>1</sup>H-NMR Titration Experiments

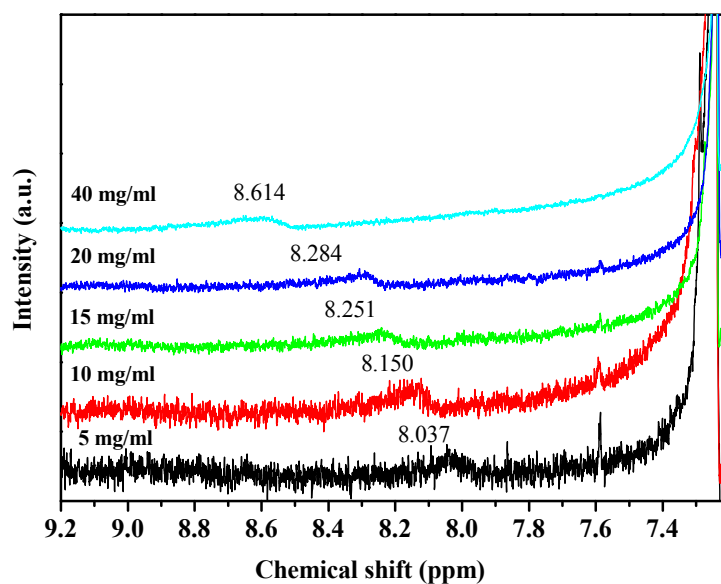


**Figure S7.** <sup>1</sup>H-NMR spectra of LR-PU31 polymer in  $\text{CDCl}_3$  with different concentrations.

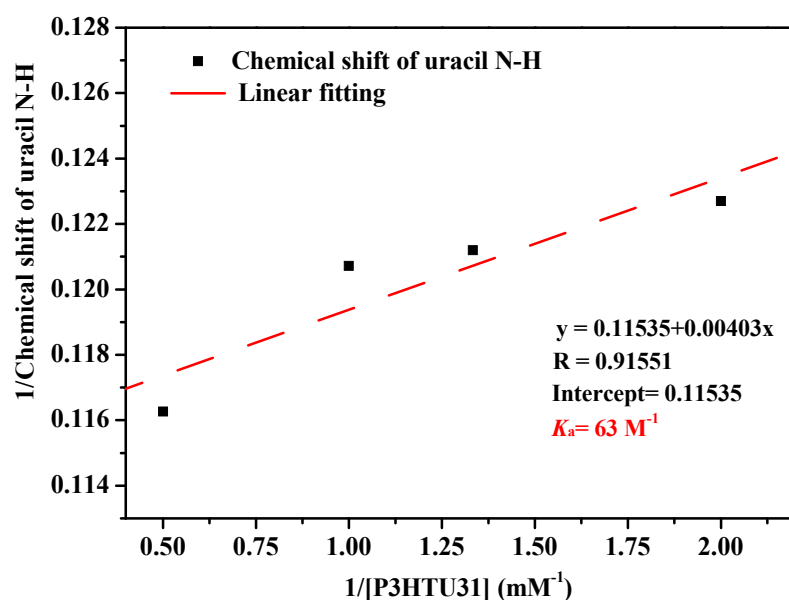


**Figure S8.** Benesi–Hildebrand plots for the LR-PU31 self-association in  $\text{CDCl}_3$  at 25 °C.

## Solvent Resistance Experiments

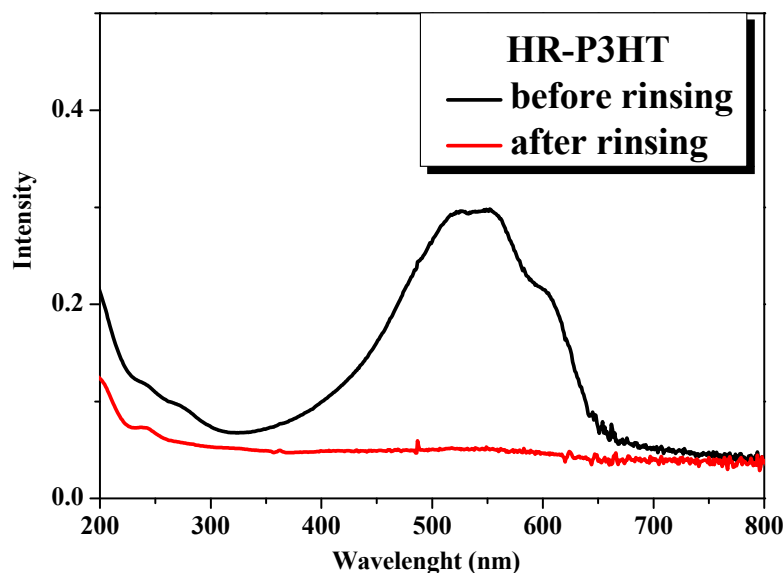


**Figure S9.** Absorption spectra of spin-coated HR-P3HT films before and after rinsing with chlorobenzene.

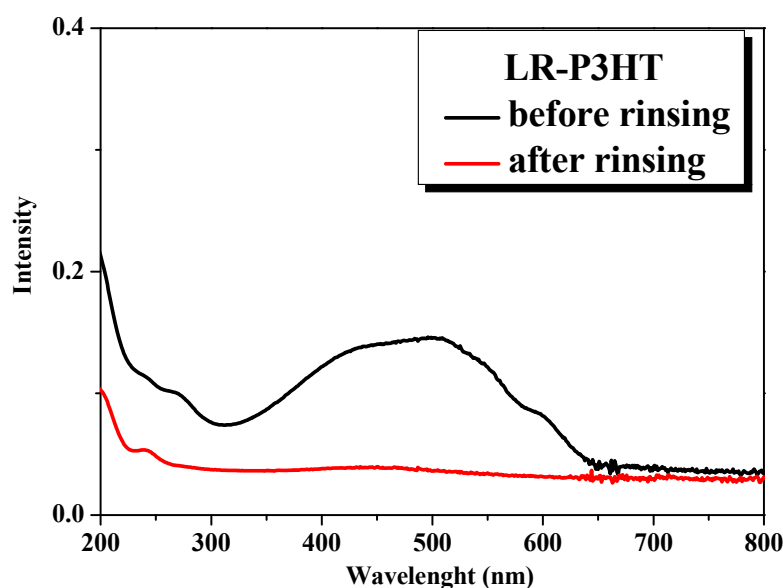


**Figure S10.** Absorption spectra of spin-coated LR-P3HT films before and after rinsing with chlorobenzene.

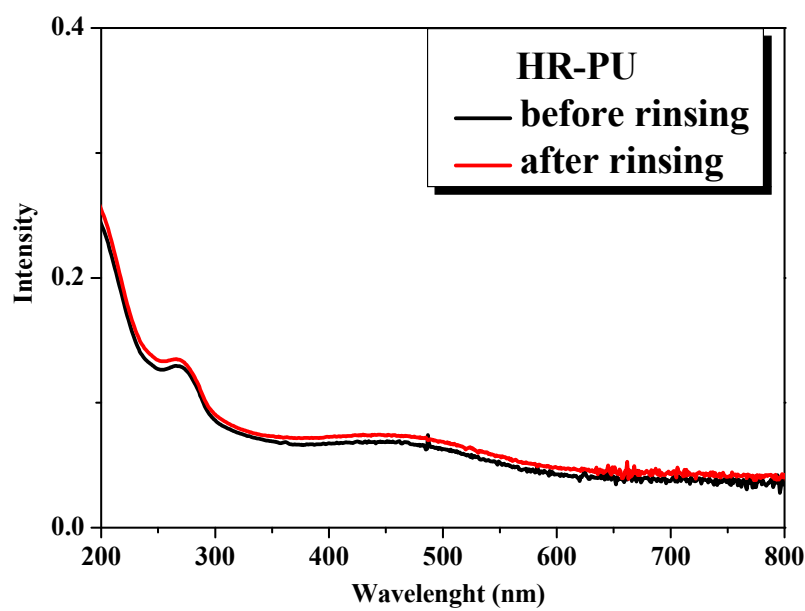


**Figure S11.** Absorption spectra of spin-coated HR-PU films before and after rinsing with chlorobenzene.

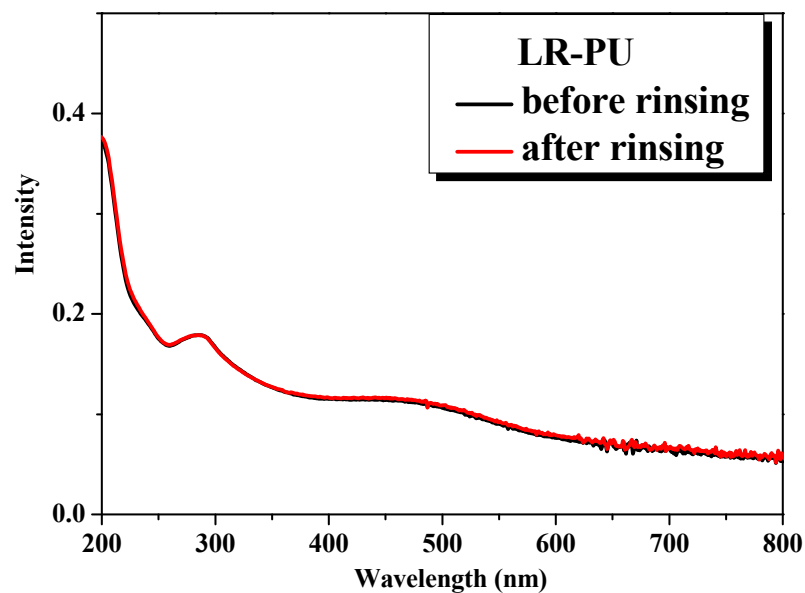


**Figure S12.** Absorption spectra of spin-coated LR-PU films before and after rinsing with chlorobenzene.

## OLED Devices

**Table S2.** Summary of energy gap ( $E_g$ ), HOMO, and LUMO for the uracil-functioned polymers, LR-P3HT and HR-P3HT.

HITMs	$E_g^a$ (eV)	HOMO <sup>b</sup> (eV)	LUMO <sup>c</sup> (eV)
RR-P3HT	2.04	-5.19	-3.15
LR-P3HT	1.86	-5.19	-3.33
LR-PU31	2.50	-5.36	-2.86
LR-PU	2.28	-5.12	-2.84
RR-PU	2.19	-5.17	-2.98

<sup>a</sup>  $E_g$  was obtained from the UV-vis absorption spectra and cyclic voltammetry.

<sup>d</sup> HOMO =  $E_{ox,\text{onset}} + 4.8$  eV

<sup>c</sup> LUMO = HOMO -  $E_g$ .

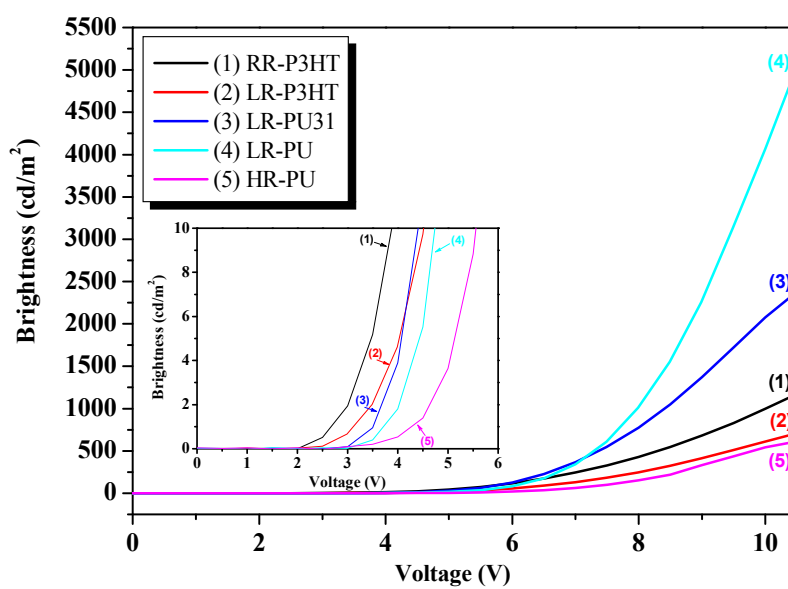


**Figure S13.** Voltage–luminance ( $V$ – $L$ ) characteristics of devices having the configurations ITO/HITL/Alq<sub>3</sub>/LiF/Al.

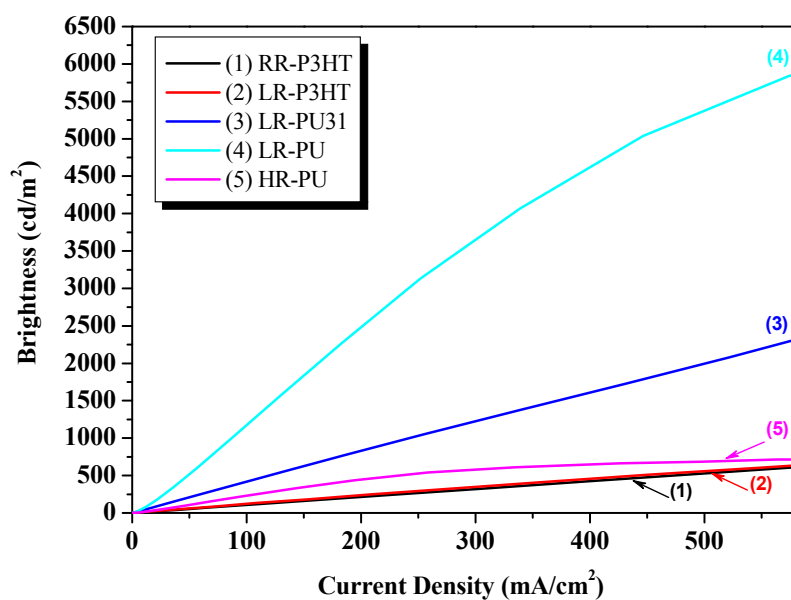


**Figure S14.** Current density–luminance ( $I$ – $L$ ) characteristics of devices having the configurations ITO/HITL/Alq<sub>3</sub>/LiF/Al.

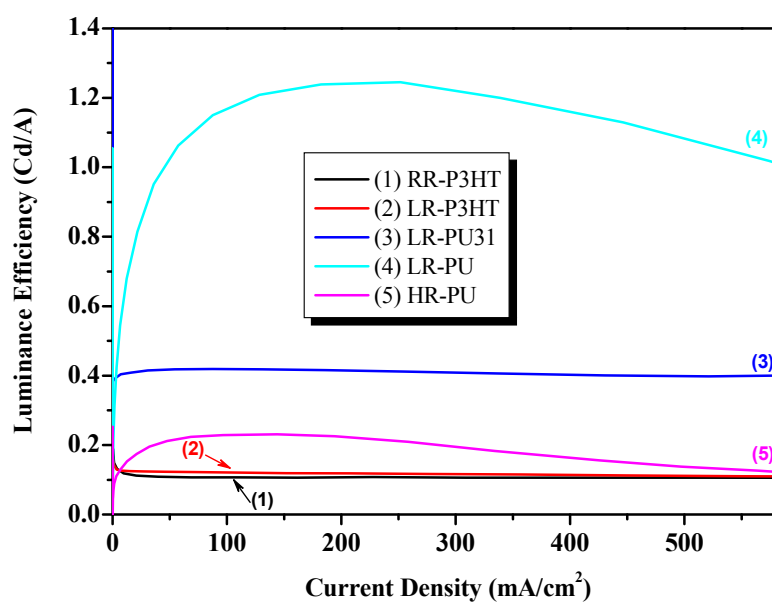


**Figure S15.** Current density–luminance efficiency characteristics of devices having the configurations ITO/HITL/Alq<sub>3</sub>/LiF/Al.

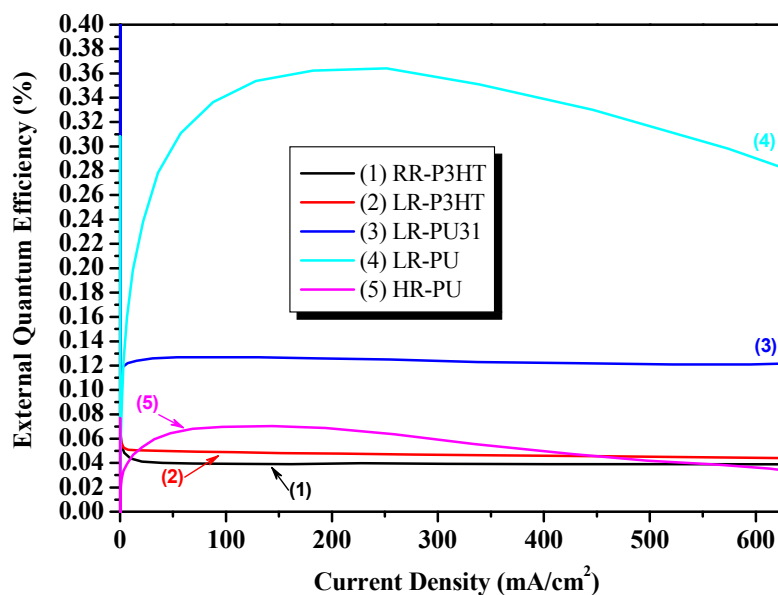


**Figure S16.** Current density–external quantum efficiency characteristics of devices having the configurations ITO/HITL/Alq<sub>3</sub>/LiF/Al.

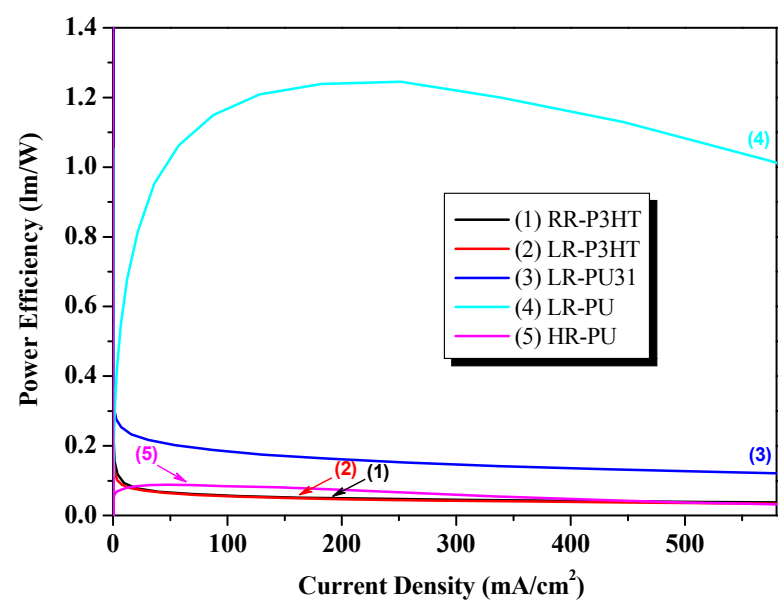


**Figure S17.** Current density–power efficiency characteristics of devices having the configurations ITO/HITL/Alq<sub>3</sub>/LiF/Al.

## References

1. Zhai, L.; Pilston, R. L.; Zaiger, K. L.; Stokes, K. K.; McCullough, R. D. *Macromolecules* **2003**, *36*, 61-64.
2. Lindsell, W. E.; Murray, C.; Preston, P. N.; Woodman, T. A. J. *Tetrahedron* **2000**, *56*, 1233-1245.